Article type: Data article

Title: Local water year values for the conterminous United States

Running title: CONUS local water years

Authors: Xinyu Sun*[1] and Kendra Spence Cheruvelil[1,2]

***Corresponding author**: Xinyu Sun (sunxiny9@msu.edu)

Affiliation:

1 Department of Fisheries and Wildlife, Michigan State University, 480 Wilson Rd, East Lansing, MI, USA 48824

2 Lyman Briggs College, Michigan State University, 919 E Shaw Ln, East Lansing, Michigan, USA 48825

Author Contribution Statement: XS and KSC conceived the project and designed the overall approach. XS collected and processed the data, wrote the code, and conducted the spatial interpolation. XS wrote the first draft of the manuscript and both authors revised the manuscript.

Submission statement: This paper is a non-peer reviewed preprint submitted to EarthArXiv.

Conflict of interest: Authors have no conflict of interest to declare.

Data Availability Statement: Local water year (LWY) data and metadata, as well as the code used to create LWY are available on the Environmental Data Initiative (EDI) Data Portal at https://doi.org/10.6073/pasta/94185d860444092a1d358d02dbc6bb40. The total annual precipitation data used for making the maps are available on GitHub at https://github.com/viola18/local-water-year-precipitation-data.

Abstract:

Quantifying and predicting precipitation and its influence on ecosystems is challenged by the asynchrony between precipitation and water fluxes. To account for this asynchrony, scientists and managers use "water year" to estimate precipitation and its impacts on water flow and ecosystems. However, traditional water year definitions either do not consider areal variation in climate and hydrology or cannot be applied at the regional or continental scale. Using an existing definition whereby the water year begins in the month with the lowest average monthly streamflow, we developed a local water year (LWY) that considers spatial variation and can be applied at the continental scale. We employed a spatial interpolation technique to assign LWY start and end months to 202 subregions across the conterminous U.S. that range from 4,384 to 134,755 km^2. This dataset can be linked with diverse climate, terrestrial, and aquatic data for broad-scale studies.

Keywords: Water year; Streamflow; Spatial variation; Spatial interpolation; Macroscale; Precipitation

Background & Motivation

Precipitation plays a crucial role in shaping ecosystems. As a result of climate change, there has been greater interannual variability in precipitation in many regions worldwide (IPCC 2021), causing increased frequency and intensity of extreme events such as drought and flooding (Easterling et al. 2000; Grimm & Natori 2006; Prein et al. 2016; Kundzewicz et al. 2020). In addition, precipitation is highly spatially variable, especially when considering macroscale spatial extents of regions to continents (Mock 1996; Augustine 2010). Despite such spatial and temporal variation in precipitation, a calendar year timeframe (from January 1st to December 31st) has often been used to examine and predict the impacts of precipitation and relevant extreme events on aquatic systems. The use of the calendar year is challenged by the fact that water fluxes are sometimes asynchronous with precipitation. For example, rainfall in late fall can be retained in the soil and influence water fluxes the following spring, which is not captured when using a calendar year (Pike 1964; Kamps & Heilman 2018).

To account for this asynchrony between precipitation and water flow, researchers adopted a "water year" that usually spans two standard calendar years. For example, the U.S. Geological Service (USGS) water year, which was adopted a century ago, starts on October 1st and ends on September 30th of the next year (Henshaw et al. 1915). This USGS water year is applied to the whole U.S. and intends to account for the influence of snowfall from October to December on the next year's streamflow (Henshaw et al. 1915). However, different regions of the U.S. have different timing of precipitation (including snowfall) and hydrology, as well as varying topographic patterns, all of which affect relationships between (and timing of) precipitation and water fluxes (Nicótina et al. 2008; Condon & Maxwell 2015; Torre Zaffaroni et al. 2023). These facts mean that a more localized timeframe is needed rather than applying a single water year to the macroscale.

Researchers' definitions for water year, and the subsequent start/end times of that water year, have depended on the locations, ecosystem types, and research questions. For example, Olson et al. (2013) started their water year in April when analyzing the methane and carbon dioxide fluxes of a temperate peatland, and Kamps and Heilman (2018) started their water year in September to match annual precipitation with water and carbon budget in Central Texas. These (and other) studies use water years for a relatively local spatial extent (e.g., watershed or U.S. state). However, organisms and ecological processes are influenced by multi-scale factors, from local (e.g., lake morphometry) to regional (e.g., land use) and macroscale (e.g., climate), and these factors can sometimes interact to affect ecosystems (Heffernan et al. 2014; Rose et al. 2017; LaRue et al. 2021). Thus, it is crucial to investigate and predict how ecosystems respond to environmental changes, such as precipitation variability and relevant extreme climatic events, across multiple spatial and temporal scales.

The need for macroscale research highlights the lack of a localized water year timeframe that can be applied at a broader, regional to continental scale. One challenge to doing so has been the limited data for variables such as snow melting time, ice-off dates, and annual gross primary productivity (e.g., Olson et al. 2013, Kamps & Heilman 2018). However, Wasko et al. (2020) proposed a climate- and hydrology-relevant local water year (LWY) timeframe that solely used streamflow data that are available for most areas globally. This LWY provides a site-specific timeframe beginning in the month with the lowest average monthly streamflow to capture the concurrent and lagged associations between precipitation and hydrology (Wasko et al. 2020). Using this localized timeframe, they predicted the timing and trends of flooding and streamflow at the global scale and demonstrated an improved accuracy of estimation compared with using a calendar year timeframe (Wasko et al. 2020).

Although a big step forward for global studies relying on water year data, these data do not completely cover the conterminous U.S. (CONUS), which may limit regional to CONUS-scale research. Thus, we build on their work by extending this local water year timeframe to cover all the areas in the CONUS. We used recent (1990 to 2018) streamflow data, the same method used by Wasko et al. (2020), and a spatial interpolation method to construct a CONUS-scale LWY timeframe. To create this LWY, we used regions that were created based on the drainage features by the USGS (Seaber et al. 2007). This hierarchical regionalization framework divides and subdivides the U.S. into successively smaller hydrologic units (HUs) and we chose to use the HU4 subregion, which is the second-level classification that delineates large river basins (USGS 2024). There are 202 HU4s in the CONUS that range in area from 4,384 to - 134,755 km^2. These LWY data created for subregions of the U.S. will help advance understanding of the impacts of variability in precipitation and streamflow on inland waters at a macroscale.

Data Description

This data product consists of two datasets housed on the Environmental Data Initiative (EDI) repository (https://doi.org/10.6073/pasta/94185d860444092a1d358d02dbc6bb40), as well as our R code (file name: local water year.R). The first dataset (file name: water year 1045 sites.csv) was used to develop and evaluate the LWY end month across the CONUS. This file includes the identifier from the Global Runoff Data Centre, which is the archive where we obtained streamflow data ("grdc_no" column), end month of the LWY ("wy.month" column), and locational information (longitude (“lon” column), latitude (“lat” column), altitude (“altitude” column), and the name of the river (“river” column) and station (“station” column) of each gauging site where the daily streamflow data were measured (the process of site selection will be described in the next section). There are a total of 1045 sites, and the most common LWY end month among these sites is July (273 sites), followed by August (240 sites), December (172 sites), January (103 sites), and September (80 sites) (Figure 1a, 2a).

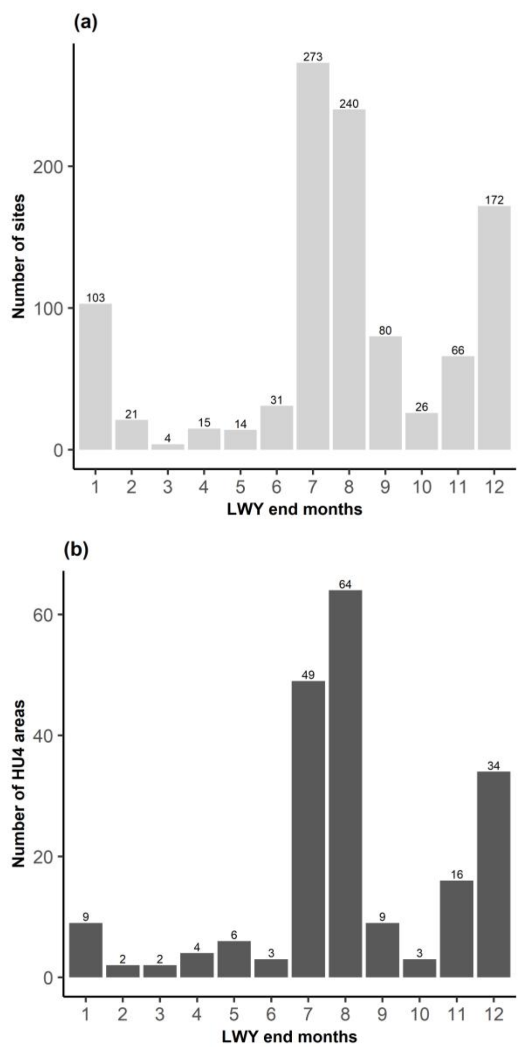

Figure 1. The number of sites (a) and subregions (b) by LWY end months. Subregion = HU4 (Seaber et al. 2007).

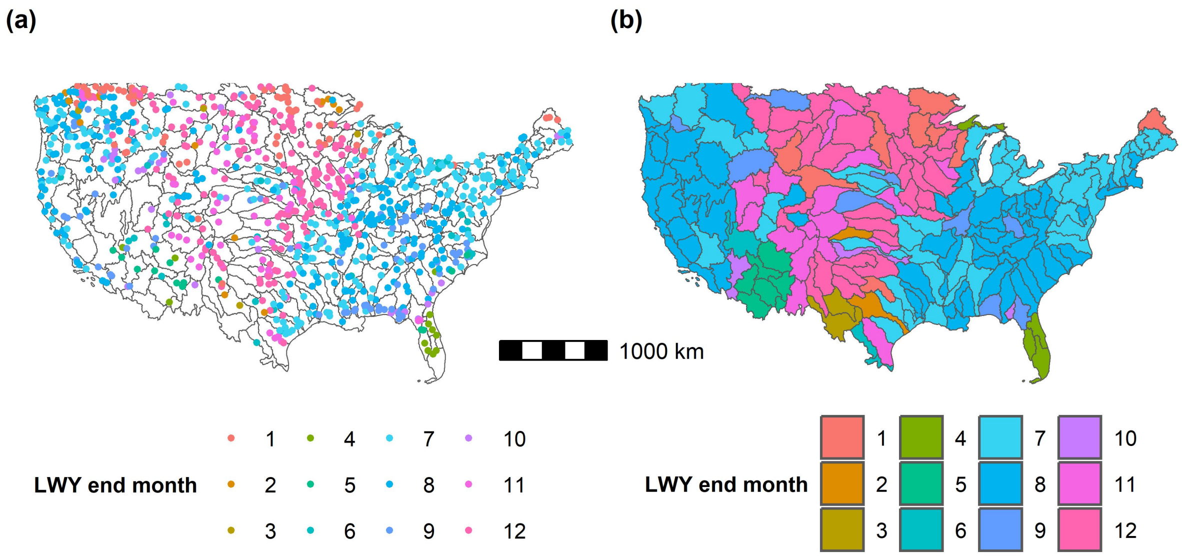

Figure 2. Maps showing the local water year (LWY) end month of each site overlaid with subregion polygons (a) and the end month for each subregion (b). In plot (a), there are 17 subregions without streamflow data. Colors represent the end months. Subregion = HU4 (Seaber et al. 2007). More information about HU4s can be found on the USGS website: https://water.usgs.gov/GIS/huc.html

The second dataset (file name: hu4 water year with notes.csv) contains the local water year data for each subregion. This file includes the start ("start.month" column) and end month ("end.month" column) of the LWY for each of the 202 subregions (i.e., 4-digit Hydrologic Unit; HU4) across the CONUS ("hu4.code" column). This dataset also includes a "notes" column that provides details about whether there were streamflow data in the subregion and the method we used to manually determine the LWY end month. There are three categories in this column: 1) dominant, which indicates that there were streamflow data and a single dominant LWY end month value in the subregion, based on which the end month was chosen; 2) Dec_Jan_interpolation, which indicates that there were streamflow data but had multiple, different LWY end month values in the subregion, and the decision was made by checking the original site-specific streamflow data; and 3) ND_interpolation, which indicates that there was no streamflow data in the area and the end month was determined based on the dominant LWY end month value. More details about the methodology can be found in sections 3 and 4.

The results of this work are 202 LWYs, one for each subregion across the CONUS. There are spatial differences in LWY end months (Figure 2b). For example, along the eastern and western edges of the CONUS, the LWY usually ends in July or August, except for the very southeast where it ends in April. In contrast, there is much more heterogeneity in LWY in the central U.S., with November and December being the most common end months. The most common LWY end month among all subregions is August (64 areas), followed by July (49 areas), December (34 areas), and November (16 areas) (Figure 1b).

Methods

We generated subregion-specific LWYs based on the definition and method proposed by Wasko et al. (2020), in combination with daily streamflow data and spatial interpolation. Data processing was performed in R (R Core Team 2023).

We used daily streamflow data from the Global Runoff Data Centre (GRDC; GRDC 2023) to calculate the monthly streamflow at each site (i.e., river gauge station). The GRDC is an open-access archive of international data that has been widely used in regional, multinational, and global hydrological studies (e.g., Hong et al. 2007; Wasko et al. 2021; Brunner & Slater 2022). We first downloaded data from 1990 to 2018 for the CONUS. Then, we filtered the streamflow data for sites that met four criteria to avoid big missing gaps in data, to take into account potential interannual variation in streamflow features, and to ensure that the data are relatively 'recent': 1) with at least 10 years of data, 2) with at least eight months of data from at least half of the years, 3) average daily streamflow data missing rate was ≤ 80% across all the years, and 4) the last year of data is post-2000. This process resulted in 1,045 sites spread across the CONUS.

Next, for each site, we calculated the average monthly streamflow data and compared these monthly averages to determine the month with the lowest streamflow. This month became the start month of a site's LWY (i.e., each site has its own lowest-streamflow-month, which is the start month of an LWY; Wasko et al. 2020). Interestingly, although a previous study suggested that low-river-flow timing in some European and U.S. regions exhibit slight interannual variation (Floriancic et al. 2021), the end month of the LWY was consistent from 1990 to 2018 across all the sites in our dataset.

We then applied ordinary kriging to interpolate site (river gaging station) LWY end month data (months as integers, 1 through 12) to the whole CONUS using gstat (v2.1-1, Pebesma & Graeler 2023) and raster (v3.6-23, Hijmans et al. 2023) R packages. Ordinary kriging (OK) is a geostatistical technique commonly used to interpolate and map data for unsampled locations and areas (e.g., Sanabria et al. 2013; Boudibi et al. 2019; Li et al. 2023). OK generally involves three steps: computing the semivariogram, defining a semivariogram model, and interpolating based on the semivariogram model (Gimond 2023).

We computed the semivariogram, which depicts the spatial correlation between the neighboring values, using equation (1),

$$\gamma(h) = \frac{1}{2n}\sum_{i=1}^{n} [\mathrm{Z}(\mathrm{x_i}) - \mathrm{Z}(\mathrm{x_i} + \mathrm{h})]^2 \qquad (1)$$

where $\gamma(h)$ is the semivariogram; $Z(x_i)$ and $Z(x_i + h)$ are the data at locations x_i and $x_i + h$, respectively; and n is the number of pairs of data separated by distance h (Li & Heap 2011; Sanabria et al. 2013). Second, we fit a mathematical model to the semivariogram. The spherical function was used in our model, and we adjusted parameter values (e.g., partial sill, range, and nugget) to improve the model fit. Third, we applied this semivariogram model to interpolate the LWY end-month data, by using equations (2) and (3) to estimate the local data (at the unsampled location) using neighboring data,

$$Z^*(x_0) = \sum_{i=1}^{n} \lambda_i Z(x_i) \qquad (2)$$

$$var\{Z^*(x_0) - Z(x_0)\} = \text{minimum} \qquad (3)$$

where $Z^*(x_0)$ is the estimated value at location x_0; $Z(x_i)$ is the data value at location x_i; and λ_i is the weighting factor that is determined by minimizing the variance (equation 3). Finally, we overlaid the interpolated end month LWY values with subregion polygons for the CONUS to assign the LWY end month for each subregion.

The resulting 202 subregion LWYs include 156 subregions that are labeled "dominant" in the dataset (hu4 water year with notes.csv, "notes" column). These subregions had streamflow data and a single dominant LWY end month in the subregion, so the end month was chosen based on the dominant value. There are 29 subregions labeled as "Dec_Jan_interpolation", which indicates that there were streamflow data but multiple different LWY end month values in the subregion. The decision of LWY end month of the subregion was made by checking the original site-specific LWY data and determining the dominant month. For the 17 subregions without streamflow data and were labeled "ND_interpolation", the month was determined solely based on interpolation results and the dominant interpolated LWY end month value.

Technical Validation

We assessed the performance of the spatial interpolation method using a leave-one-out cross-validation approach (Sanabria et al. 2013). Firstly, we randomly chose a site (i.e., river gaging station) and removed its LWY data from the dataset. Then, we applied the ordinary kriging method described above to the new dataset, re-estimated the LWY end month of the removed site, and compared the new estimated LWY end month value with the actual end month. We repeated this process 10 times on 10 different, spatially-separated sites. We found that the estimated and the actual end month of these 10 sites were either the same or differed by one month (mean absolute difference = 0.4 months), depending on the streamflow data density of the subregion. Subregions with a higher data density had higher accuracies than areas with a lower density of data.

Data Use and Recommendations for Reuse

This local water year dataset is intended to provide a localized, continental-scale timeframe that can be used for studying the features and impacts of precipitation and hydrology at various spatial scales in the CONUS. Here, we provide an example of using this LWY timeframe to identify the water years with the lowest and highest total annual precipitation from LWYs 2009 to 2018. We obtained monthly precipitation data from calendar years January 2008 to December 2018 from the LAGOS-US GEO module (Smith et al. 2022) and used these data to calculate the total annual precipitation (TAP) value for 3,000 randomly selected lakes (out of 479,950 lakes) across the CONUS. We assigned each of these lakes an LWY end month according to the subregion they are located in (i.e., all the lakes in the same subregion share the same end month; Sun & Cheruvelil 2024), and then calculated annual precipitation based on that LWY timeframe. For comparison, we calculated the lake-specific TAP based on the USGS water year that ends on September 30th. For both timeframes, the water year is named by the calendar year in which it ends (e.g., the 12-month period from August 1st, 2010 to July 31st, 2011 = LWY

2011). The water years with the lowest and highest annual precipitation were the same for some lakes (e.g., lakes' lowest TAP years in California) using the two timeframes, but were different for others (e.g., lakes' highest TAP years in Florida) (Figure 3). Thus, different TAPs could be calculated using the two water year definitions, which may further affect the identification of drought or flooding years and the estimation and prediction of precipitation impacts, suggesting that using a localized LWY for macroscale research could be more appropriate than a single water year. This LWY dataset considers areal variations and can be used in various meteorological, hydrological, and ecological studies to identify and predict trends in precipitation, extreme events (drought and flooding), and water fluxes as well as investigate their effects on ecosystems (e.g., Kamps & Heilman 2018) and human communities (e.g., calculating hydropower generation capacity; Bongio et al. 2016).

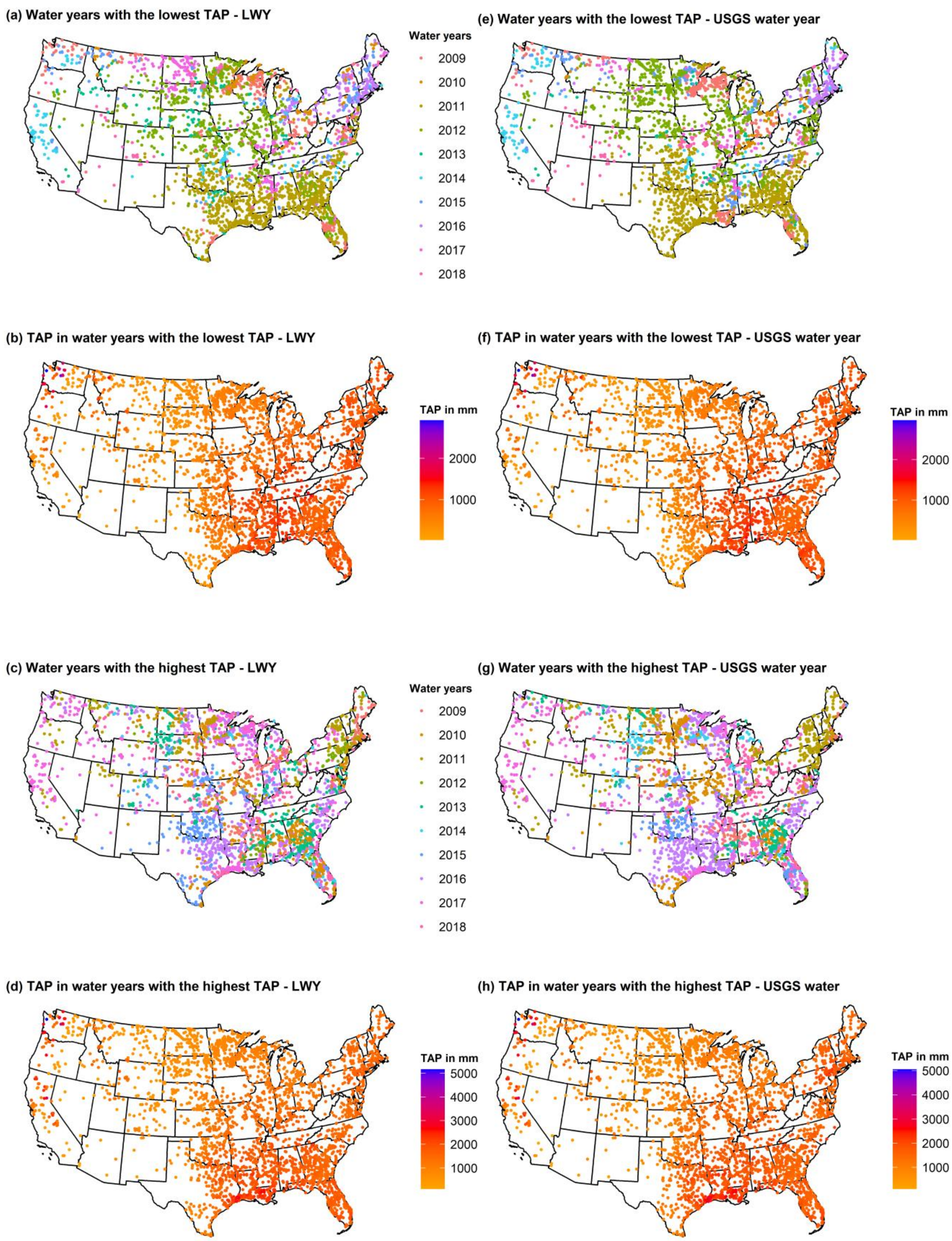

Figure 3. Maps showing the water years (a, c, e, and g) and the total annual precipitation (TAP) in the water years (b, d, f, and h) with the lowest and highest TAP of each lake by state. Plots (a) to (d) used the LWY time frame herein and plots (e) to (h) used the USGS water year timeframe.

Future users of the subregion-specific LWYs can combine these data with a wide range of climatic, as well as terrestrial and aquatic abiotic and biotic data, by linking our dataset with other data products, such as LAGOS-US modules (e.g., Cheruvelil et al. 2021) or USGS datasets (e.g., Blodgett 2023) using subregion identifiers (i.e., HU4 codes). Moreover, our R code is available for download at the EDI repository so that users can apply a similar method to other regions around the world to generate site or region-specific LWY timeframes. As such, these data will be a valuable addition to the literature that can contribute to building macroscale understanding of precipitation and streamflow variability and their influences on a variety of systems.

Acknowledgments: We thank Dr. Conrad Wasko and his colleagues for kindly guiding us on how to download data from GRDC and sharing data with us. This work was supported by the U.S. National Science Foundation (NSF) Macrosystems Biology & NEON-Enabled Science Program (DEB #1638679).

References

Augustine, D. J. (2010). Spatial versus temporal variation in precipitation in a semiarid ecosystem. *Landscape Ecology*, *25*(6), 913–925. https://doi.org/10.1007/s10980-010-9469-y

Blodgett, D. L. (2023). *Twelve-digit hydrologic unit soil moisture, recharge, actual evapotranspiration, and snowpack water equivalent storage from the National Hydrologic Model Infrastructure with the Precipitation-Runoff Modeling System 1980-2016*. https://doi.org/10.5066/P9W148A1

Bongio, M., Avanzi, F., & De Michele, C. (2016). Hydroelectric power generation in an Alpine basin: Future water-energy scenarios in a run-of-the-river plant. *Advances in Water Resources*, *94*, 318–331. https://doi.org/10.1016/j.advwatres.2016.05.017

Boudibi, S., Sakaa, B., & Zapata-Sierra, A. J. (2019). Groundwater quality assessment using GIS, ordinary kriging and WQI in an arid area. *PONTE International Scientific Researchs Journal*, *75*(12). https://doi.org/10.21506/j.ponte.2019.12.14

Brunner, M. I., & Slater, L. J. (2022). Extreme floods in Europe: Going beyond observations using reforecast ensemble pooling. *Hydrology and Earth System Sciences*, *26*(2), 469–482. https://doi.org/10.5194/hess-26-469-2022

Cheruvelil, K. S., Soranno, P. A., McCullough, I. M., Webster, K. E., Rodriguez, L. K., & Smith, N. J. (2021). LAGOS-US LOCUS v1.0: Data module of location, identifiers, and physical characteristics of lakes and their watersheds in the conterminous U.S. *Limnology and Oceanography Letters*, *6*(5), 270–292. https://doi.org/10.1002/lol2.10203

Condon, L. E., & Maxwell, R. M. (2015). Evaluating the relationship between topography and groundwater using outputs from a continental-scale integrated hydrology model. *Water Resources Research*, *51*(8), 6602–6621. https://doi.org/10.1002/2014WR016774

Easterling, D. R., Meehl, G. A., Parmesan, C., Changnon, S. A., Karl, T. R., & Mearns, L. O. (2000). Climate extremes: Observations, modeling, and impacts. *Science*, *289*(5487), 2068–2074. https://doi.org/10.1126/science.289.5487.2068

Floriancic, M. G., Berghuijs, W. R., Molnar, P., & Kirchner, J. W. (2021). Seasonality and drivers of low flows across Europe and the United States. *Water Resources Research*, *57*(9), e2019WR026928. https://doi.org/10.1029/2019WR026928

Gimond, M. (2023). *Intro to GIS and spatial analysis*. https://mgimond.github.io/Spatial/index.html.

GRDC. (2023). *GRDC - The Global Runoff Data Centre*. https://grdc.bafg.de/GRDC/EN/Home/homepage_node.html

Grimm, A. M., & Natori, A. A. (2006). Climate change and interannual variability of precipitation in South America. *Geophysical Research Letters*, *33*(19), 2006GL026821. https://doi.org/10.1029/2006GL026821

Heffernan, J. B., Soranno, P. A., Angilletta, M. J., Buckley, L. B., Gruner, D. S., Keitt, T. H., Kellner, J. R., Kominoski, J. S., Rocha, A. V., Xiao, J., Harms, T. K., Goring, S. J., Koenig, L. E., McDowell, W. H., Powell, H., Richardson, A. D., Stow, C. A., Vargas, R., & Weathers, K. C. (2014). Macrosystems ecology: Understanding ecological patterns and processes at continental scales. *Frontiers in Ecology and the Environment*, *12*(1), 5–14. https://doi.org/10.1890/130017

Hendrickson, W. A., & Ward, K. B. (1975). Atomic models for the polypeptide backbones of myohemerythrin and hemerythrin. *Biochemical and Biophysical Research Communications*, *66*(4), 1349–1356. https://doi.org/10.1016/0006-291x(75)90508-2

Henshaw, F. F., Baldwin, G. C., Stevens, G. C., & Fuller, E. S. (1915). *Surface water supply of the United States, 1911* (Water Supply Paper). U.S. Geological Service. https://doi.org/10.3133/wsp312

Hijmans, R. J., Etten, J. van, Sumner, M., Cheng, J., Baston, D., Bevan, A., Bivand, R., Busetto, L., Canty, M., Fasoli, B., Forrest, D., Ghosh, A., Golicher, D., Gray, J., Greenberg, J. A., Hiemstra, P., Hingee, K., Ilich, A., Geosciences, I. for M. A., … Wueest, R. (2023). *raster: Geographic Data Analysis and Modeling* (3.6-23). https://cran.r-project.org/web/packages/raster/index.html

Hong, Y., Adler, R. F., Hossain, F., Curtis, S., & Huffman, G. J. (2007). A first approach to global runoff simulation using satellite rainfall estimation. *Water Resources Research*, *43*(8), 2006WR005739. https://doi.org/10.1029/2006WR005739

Intergovernmental Panel On Climate Change. (2021). *Climate Change 2021 – The Physical Science Basis: Working Group I Contribution to the Sixth Assessment Report of the Intergovernmental Panel on Climate Change*. Cambridge University Press. https://doi.org/10.1017/9781009157896

Kamps, R. H., & Heilman, J. L. (2018). A method to calculate a locally relevant water year for ecohydrological studies using eddy covariance data. *Ecohydrology*, *11*(7), e1980. https://doi.org/10.1002/eco.1980

Kidder, G. W., & Montgomery, C. W. (1975). Oxygenation of frog gastric mucosa in vitro. *The American Journal of Physiology*, *229*(6), 1510–1513. https://doi.org/10.1152/ajplegacy.1975.229.6.1510

Kundzewicz, Z. W., Huang, J., Pinskwar, I., Su, B., Szwed, M., & Jiang, T. (2020). Climate variability and floods in China - A review. *Earth-Science Reviews*, *211*, 103434. https://doi.org/10.1016/j.earscirev.2020.103434

LaRue, E. A., Rohr, J., Knott, J., Dodds, W. K., Dahlin, K. M., Thorp, J. H., Johnson, J. S., Rodríguez González, M. I., Hardiman, B. S., Keller, M., Fahey, R. T., Atkins, J. W., Tromboni, F., SanClements, M. D., Parker, G., Liu, J., & Fei, S. (2021). The evolution of macrosystems biology. *Frontiers in Ecology and the Environment*, *19*(1), 11–19. https://doi.org/10.1002/fee.2288

Li, J., & Heap, A. D. (2011). A review of comparative studies of spatial interpolation methods in environmental sciences: Performance and impact factors. *Ecological Informatics*, *6*(3–4), 228–241. https://doi.org/10.1016/j.ecoinf.2010.12.003

Li, L., Sun, J., Wang, H., Ouyang, Y., Zhang, J., Li, T., Wei, Y., Gong, W., Zhou, X., & Zhang, B. (2023). Spatial distribution and temporal trends of dietary niacin intake in Chinese residents ≥ 5 years of age between 1991 and 2018. *Nutrients*, *15*(3), 638. https://doi.org/10.3390/nu15030638

Mock, C. J. (1996). Climatic controls and spatial variations of precipitation in the western United States. *Journal of Climate*, *9*(5), 1111–1125. https://doi.org/10.1175/1520-0442(1996)009<1111:CCASVO>2.0.CO;2

Nicótina, L., Alessi Celegon, E., Rinaldo, A., & Marani, M. (2008). On the impact of rainfall patterns on the hydrologic response. *Water Resources Research*, *44*(12), 2007WR006654. https://doi.org/10.1029/2007WR006654

Olson, D. M., Griffis, T. J., Noormets, A., Kolka, R., & Chen, J. (2013). Interannual, seasonal, and retrospective analysis of the methane and carbon dioxide budgets of a temperate peatland. *Journal of Geophysical Research: Biogeosciences*, *118*(1), 226–238. https://doi.org/10.1002/jgrg.20031

Pebesma, E., & Graeler, B. (2023). *gstat: Spatial and Spatio-Temporal Geostatistical Modelling, Prediction and Simulation* (2.1-1). https://github.com/r-spatial/gstat/

Pike, J. G. (1964). The estimation of annual run-off from meteorological data in a tropical climate. *Journal of Hydrology*, *2*(2), 116–123. https://doi.org/10.1016/0022-1694(64)90022-8

Prein, A. F., Holland, G. J., Rasmussen, R. M., Clark, M. P., & Tye, M. R. (2016). Running dry: The U.S. Southwest's drift into a drier climate state. *Geophysical Research Letters*, *43*(3), 1272–1279. https://doi.org/10.1002/2015GL066727

R Core Team. (2023). *R: A language and environment for statistical computing*. R Foundation for Statistical Computing. https://www.r-project.org/

Rajcáni, J., Krobová, J., & Málková, D. (1975). Distribution of Lednice (Yaba 1) virus in the chick embryo. *Acta Virologica*, *19*(6), 467–472.

Rose, K. C., Graves, R. A., Hansen, W. D., Harvey, B. J., Qiu, J., Wood, S. A., Ziter, C., & Turner, M. G. (2017). Historical foundations and future directions in macrosystems ecology. *Ecology Letters*, *20*(2), 147–157. https://doi.org/10.1111/ele.12717

Sanabria, L. A., Qin, X., Li, J., Cechet, R. P., & Lucas, C. (2013). Spatial interpolation of McArthur's forest fire danger index across Australia: Observational study. *Environmental Modelling & Software*, *50*, 37–50. https://doi.org/10.1016/j.envsoft.2013.08.012

Seaber, P. R., Kapinos, F. P., & Knapp, G. L. (2007). *Hydrologic Unit Maps*. U.S. Geological Survey. https://pubs.usgs.gov/wsp/wsp2294/

Smith, N. J., Webster, K. E., Rodriguez, L. K., Cheruvelil, K. S., & Soranno, P. A. (2022). *LAGOS-US GEO v1.0: Data module of lake geospatial ecological context at multiple spatial and temporal scales in the conterminous U.S.* Environmental Data Initiative. https://doi.org/10.6073/PASTA/0E443BD43D7E24C2B6ABC7AF54CA424A

Sun, X., & Cheruvelil, K. S. (2024). *Local water year for 4-digit hydrologic unit areas across the conterminous United States*. Environmental Data Initiative. https://doi.org/10.6073/PASTA/94185D860444092A1D358D02DBC6BB40. Last accessed in May 2024

Torre Zaffaroni, P., Baldi, G., Texeira, M., Di Bella, C. M., & Jobbágy, E. G. (2023). The timing of global floods and its association with climate and topography. *Water Resources Research*, *59*(7), e2022WR032968. https://doi.org/10.1029/2022WR032968

USGS. (2024). *Water resources of the United States: Hydrologic unit maps*. Https://Water.Usgs.Gov/GIS/Huc.Html. https://water.usgs.gov/GIS/huc.html

Wasko, C., Nathan, R., & Peel, M. C. (2020). Trends in global flood and streamflow timing based on local water year. *Water Resources Research*, *56*(8), e2020WR027233. https://doi.org/10.1029/2020WR027233

Wasko, C., Nathan, R., Stein, L., & O'Shea, D. (2021). Evidence of shorter more extreme rainfalls and increased flood variability under climate change. *Journal of Hydrology*, *603*, 126994. https://doi.org/10.1016/j.jhydrol.2021.126994